

# Study on the interaction between nonlinear wave and fixed floating box based on non-hydrostatic model

Pengyao Yang <sup>a</sup>, Yuxiang Ma\* <sup>a</sup>, Congfang Ai <sup>a</sup>

<sup>a</sup> The National Key Laboratory of Coastal and Ocean Engineering, Dalian University of Technology, Dalian, China  
E-mail: yuxma@dlut.edu.cn

## 1 INTRODUCTION

Accurate and efficient prediction of nonlinear waves interacting with structures has long been a concerned problem and is critical for the safety assessment and cost-effective design of marine structures. With the development of computer technology, numerical models based on the Navier-Stokes equations that accurately predict nonlinear wave interactions with structures have recently attracted more attention from researchers, many of which employ the volume of fluid method or the level-set method to capture the moving water-air interface. However, high computational cost of such NSE-based models limit their practical application.

In order to reduce the high computational cost of NSE-based numerical models, one can discard the air phase and use the so-called free surface equation to capture the free surface. Non-hydrostatic models are just such models incorporating the free surface equation to deal with the moving free surface. The development of non-hydrostatic models has been more than two decades, since Casulli and Stelling (1998)<sup>[1]</sup> and Stansby and Zhou (1998)<sup>[2]</sup> who simulated free surface flows by including non-hydrostatic effects. Therefore, this study analyzed the interaction between focused wave and the fixed floating box using non-hydrostatic model (Ai et al. 2022)<sup>[3]</sup> that employs the immersed boundary (IB) method to deal with fixed floating box.

## 2 GOVERNING EQUATIONS

The governing equations are the incompressible Euler equations, which can be expressed in the following forms by splitting the pressure into hydrostatic and non-hydrostatic components such that  $p = g(\eta - z) + q$

$$\frac{\partial u}{\partial x} + \frac{\partial v}{\partial y} + \frac{\partial w}{\partial z} = 0 \quad (1)$$

$$\frac{\partial u}{\partial t} + \frac{\partial u^2}{\partial x} + \frac{\partial uv}{\partial y} + \frac{\partial uw}{\partial z} = -g \frac{\partial \eta}{\partial x} - \frac{\partial q}{\partial x} \quad (2)$$

$$\frac{\partial v}{\partial t} + \frac{\partial uv}{\partial x} + \frac{\partial v^2}{\partial y} + \frac{\partial vw}{\partial z} = -g \frac{\partial \eta}{\partial y} - \frac{\partial q}{\partial y} \quad (3)$$

$$\frac{\partial w}{\partial t} + \frac{\partial uw}{\partial x} + \frac{\partial vw}{\partial y} + \frac{\partial w^2}{\partial z} = -\frac{\partial q}{\partial z} \quad (4)$$

Where  $u$ ,  $v$  and  $w$  are the velocity components in the horizontal  $x$  and  $y$  and vertical  $z$  directions, respectively,  $t$  is the time,  $p$  is the normalized pressure divided by a constant reference density,  $q$  is the non-hydrostatic pressure component, and  $g$  is the gravitational acceleration. Notably,  $\eta$  is

the free surface elevation in the free surface region and represents the piezometric head in the pressurized region.

Boundary conditions are required at all the boundaries of a 3D domain. In the free surface region,, the following kinematic boundary is specified at the moving free surface  $z = \eta(x, y, t)$

$$\frac{\partial \eta}{\partial t} + u \frac{\partial \eta}{\partial x} + v \frac{\partial \eta}{\partial y} = w \Big|_{z=\eta} \quad (5)$$

In the pressurized region, the kinematic boundary at the body surface is

$$-u \frac{\partial d}{\partial x} - v \frac{\partial d}{\partial y} = w \Big|_{z=-d} \quad (6)$$

At the impermeable bottom surface  $z = -h(x, y)$ , the kinematic boundary is

$$-u \frac{\partial h}{\partial x} - v \frac{\partial h}{\partial y} = w \Big|_{z=-h} \quad (7)$$

By integrating the continuity Eq. (1) from  $z = -h(x, y)$  to  $z = \eta(x, y, t)$  and applying Leibniz' rule together with Eqs. (5) and (7), the following free surface equation is obtained:

$$\frac{\partial \eta}{\partial t} + \frac{\partial}{\partial x} \int_{z=-h}^{z=\eta} u dz + \frac{\partial}{\partial y} \int_{z=-h}^{z=\eta} v dz = 0 \quad (8)$$

Similarly, by means of integration of the continuity Eq. (1) from  $z = -h(x, y)$  to  $z = -d(x, y)$  and considering Eqs. (6) and (7), the following global continuity equation in the pressurized region is obtained:

$$\frac{\partial}{\partial x} \int_{z=-h}^{z=-d} u dz + \frac{\partial}{\partial y} \int_{z=-h}^{z=-d} v dz = 0 \quad (9)$$

Considering the IB method is incorporated in the model and all the velocities inside the floating structure are zero, Eq. (9) can be rewritten as

$$\frac{\partial}{\partial x} \int_{z=-h}^{z=-\eta} u dz + \frac{\partial}{\partial y} \int_{z=-h}^{z=-\eta} v dz = 0 \quad (10)$$

Notably, Eq. (10) is only valid in the pressurized region and can be used to determine the piezometric head.

### 3 NUMERICAL ALGORITHMS

Before using a semi-implicit, fractional step algorithm to solve the governing equations, they are first integrated in the vertical direction based on a general vertical boundary-fitted coordinate system (Ai et al., 2014)<sup>[3]</sup>.

In the explicit projection method, the first step involves solving Eqs. (2)-(4) while disregarding the implicit contributions of the non-hydrostatic pressure, thereby yielding the intermediate velocity  $u_{i+1/2,j,k}^{n+1}$ ,  $v_{i,j+1/2,k}^{n+1}$  and  $w_{i,j,k}^{n+1}$ . In the second step, new velocities  $u_{i+1/2,j,k}^{n+1}$ ,  $v_{i,j+1/2,k}^{n+1}$  and  $w_{i,j,k}^{n+1}$  are calculated by correcting the intermediate values after including the non-hydrostatic pressure.

$$\frac{u_{i+1/2,j,k}^{n+1} - u_{i+1/2,j,k}^{n+1/2}}{\Delta t} = - \left( \frac{\partial q}{\partial x} \right)_{i+1/2,j,k}^{n+1} + f_{IBF}(u_{i+1/2,j,k}) \quad (11)$$

$$\frac{v_{i,j+1/2,k}^{n+1} - v_{i,j+1/2,k}^{n+1/2}}{\Delta t} = - \left( \frac{\partial q}{\partial y} \right)_{i,j+1/2,k}^{n+1} + f_{IBF}(v_{i,j+1/2,k}) \quad (12)$$

$$\frac{w_{i,j,k}^{n+1} - w_{i,j,k}^{n+1/2}}{\Delta t} = - \left( \frac{\partial q}{\partial z} \right)_{i,j,k}^{n+1} + f_{IBF}(w_{i,j,k}) \quad (13)$$

where  $f_{IBF}(u_{i+1/2,j,k})$ ,  $f_{IBF}(v_{i,j+1/2,k})$  and  $f_{IBF}(w_{i,j,k})$  are IB forces. For details about the explicit projection method and the implementation of the IB method, the reader can refer to Ai et al. (2018)<sup>[5]</sup>.

The non-hydrostatic pressures are determined by solving the Poisson equation, which is obtained by substituting Eqs. (11)-(13) into the continuity Eq. (1) discretized by the semi-implicit method together with the finite difference method. The resulting Poisson equation can be written in the following matrix form:

$$\mathbf{A}\mathbf{q} = \mathbf{b} \quad (14)$$

Where  $\mathbf{A}$  is a sparse coefficient matrix,  $\mathbf{q}$  is a vector of the non-hydrostatic pressure, and  $\mathbf{b}$  is a known vector related to explicit and intermediate velocities. The coefficients of the matrix  $\mathbf{A}$  are quite similar to those presented in Ai et al. (2019a)<sup>[6]</sup>. Moreover,  $\mathbf{A}$  is symmetric and contains 10 nonzero diagonals in bottom cells and 15 nonzero diagonals in other cells.

In addition, Eq. (9) and Eq. (10) are discretized by the following fully implicit finite difference method for stability.

#### 4 NUMERICAL RESULTS

In the test case, a regular wave incident on a box-shaped ship fixed in a harbor is considered. The

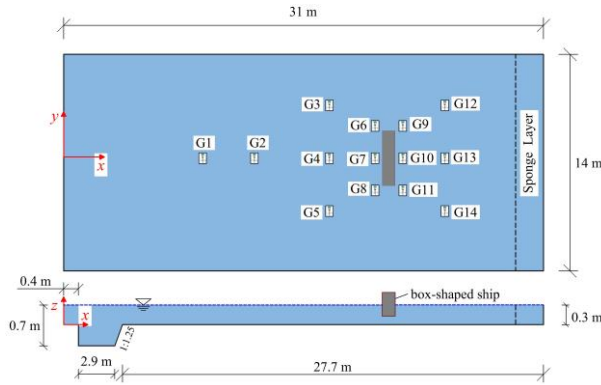


Fig. 1 Sketch of the model setup

model validation can be referred to in Ai et al. (2022)<sup>[3]</sup>. The computational domain is shown in Fig. 1, in which the floating box-shaped ship has the dimension of  $L_x = 0.6$  m,  $L_y = 2.0$  m and  $L_z = 0.45$  m and is positioned at (21.8 m, 0.0 m, 0.285 m). The draft of the ship is 0.24 m. In the working area, the still water depth is  $h = 0.3$  m. The incident focused wave with an amplitude  $H_0 = 0.03$  m and a wave period  $T_0 = 1.5$  s is specified at the left boundary of the domain. The target wave spectrum is defined by the JONSWAP spectrum with a peak enhancement

factor  $\gamma$  set to 2.2. The focus location is at the center of the structure, and the focus time is 25 s. The incident wave is generated using the dispersion-focused method.

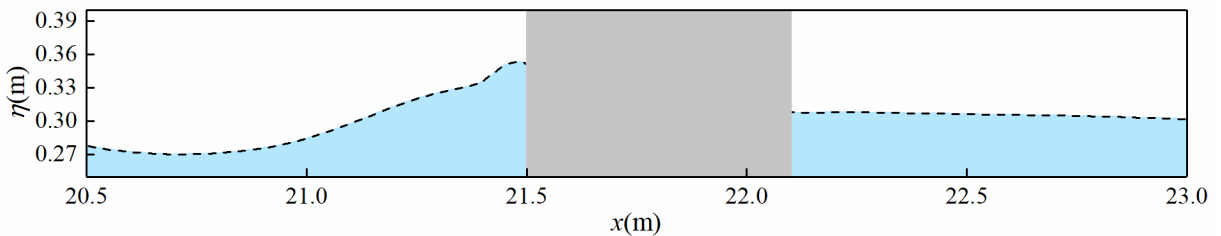


Fig. 2 Water surface of the focus time.

Fig. 2 shows the distribution of the wave surface along the x-direction ( $y = 0$ ) at the focus time, with the maximum water level observed at the front of the fixed floating box, reaching 0.358 m.

Fig 3 shows the time series of wave surface elevations in front of and behind the structure. The wave amplitude exhibits significant attenuation after passing through the fixed floating box. Fig. 4 presents time histories of the two nondimensional wave forces in the  $x$  and  $z$  directions. At the focus time, the wave forces in both directions are at their maximum.

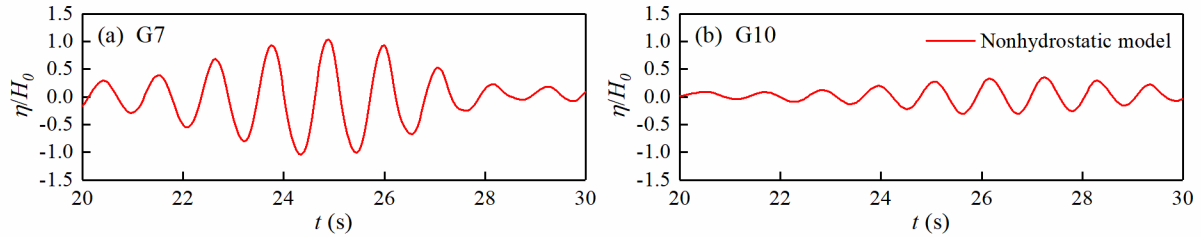


Fig. 3 Time histories of the water surface elevation.

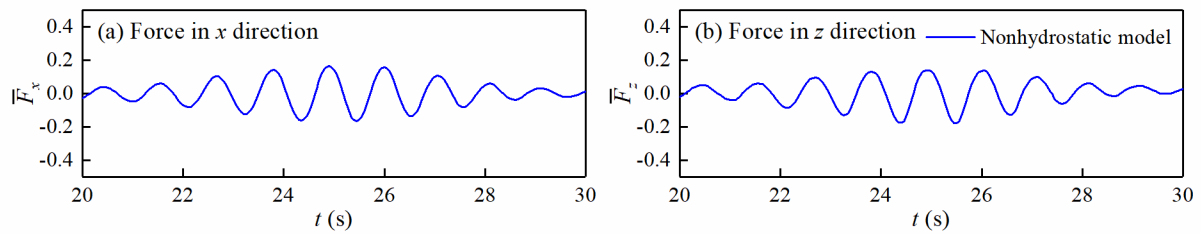


Fig. 4 The wave forces in the  $x$  and  $z$  directions

## 5 CONCLUSIONS

In this study, the interaction between the focused wave and the fixed floating box is simulated using a non-hydrostatic model. The model utilizes a semi-implicit, fractional step algorithm to solve the incompressible Euler equation and treats the free surface as a single-valued function of horizontal positions. The combination of the immersed boundary method and the global continuity equation in the pressurized region is proposed in the model, which renders an efficient solution of the Poisson equation. The computational analysis reveals that when the focused wave acts on the structure, the maximum wave run-up occurs at the front of the fixed floating box at the focus time, with a value of approximately  $2H_0$ , and the wave forces also reach their maximum.

## REFERENCES

- [1] Casulli, V., Stelling, G.S., 1998. Numerical simulation of 3D quasi-hydrostatic, free surface flows. *J. Hydraul. Eng.-ASCE* 124, 678–686.
- [2] Stansby, P.K., Zhou, J.G., 1998. Shallow-waterflow solver with non-hydrostatic pressure: 2D vertical plane problems. *Int. J. Numer. Methods Fluid.* 28, 514–563.
- [3] Ai, C., Ma, Y., Yuan, C., Xie, Z., Dong, G., Stoesser, T., 2022. An efficient 3d non-hydrostatic model for predicting nonlinear wave interactions with fixed floating structures. *Ocean Eng.* 248, 110810.
- [4] Ai, C., Ding, W., Jin, S., 2014. A general boundary-fitted 3D non-hydrostatic model for nonlinear focusing wave groups. *Ocean. Eng.* 89, 134–145.
- [5] Ai, C., Ma, Y., Yuan, C., Dong, G., 2018. Semi-implicit non-hydrostatic model for 2D nonlinear wave interaction with a floating/suspended structure. *Eur. J. Mech. B Fluid* 72, 545–560.
- [6] Ai, C., Ma, Y., Yuan, C., Dong, G., 2019a. Development and assessment of semi-implicit nonhydrostatic models for surface water waves. *Ocean Model.* 144, 101489.